

Thrust Calculation of Transverse Flux Linear Motor Considering end Effect of Motor

J.Y. Lee¹, Jung-Pyo Hong¹, Do-Hyun Kang²

¹ Department of Electrical Engineering, Changwon National University
#9 Sarimdong, Changwon, Gyeongnam, 641-773, Korea, Tel: (+8255)2625966, Fax: (+8255) 2639956

² Department of Mechatronics, Korea Electrotechnology Research Institute
#28-1, Seongjudong, Changwon, Gyeongnam, 641-120, Korea, Tel: (+8255)2603834
E-mail: jyecad@korea.com, jphong@changwon.ac.kr, dhkang@keri.re.kr

I. INTRODUCTION

Transverse Flux Linear Motor (TFLM) has so high power density per unit volume that it can reduce weight and volume of vibrator systems, and be substituted for hydraulic vibrator systems, which have disadvantages of huge size and management [1]. For design and performance assessment, however, the analysis of TFLM is more difficult than that of rotary counterparts, or the results can be inaccurate because of the end effect by limited mover length. Moreover, it is required to employ 3-dimensional (3D) analysis because of the magnetically complicated and nonsymmetrical configuration.

Therefore, this paper deals with thrust calculation of a Permanent Magnet type TFLM for a two-phase vibrator. Since this motor is used for low speed and high thrust, static thrust can also be useful data to estimate the performance of vibrator. The static thrust is calculated by 3D EMCN. For TFLM as a linear motor, the analysis method is more useful and proper than 3D FEM because of the hexahedral elementary shape and relatively fast solving time [2][3].

Considering accuracy and time required for the analysis, the vibrator is too long to model the whole construction or even only mover so that the portion of two stator-pole pitch is taken as the 3D analysis model. The end effect of mover, however, cannot be considered in the model. Therefore, Multiple-ratio is required to be multiplied by the 3D analysis results as a kind of an adjustment factor. This ratio can be obtained by the analysis of 2D model with imaginary magnetic flux path [4] to consider the 3D flux path of TFLM. The 2D analysis model does not need to have the whole shape. It is enough to model the mover and a little longer stator, which is long enough to consider the mover-end leakage flux. The Multiple-ratio is not equal to either length ratio or pole ratio of analysis model to actual model. The calculated results are compared with the measurements to verify the validity of the analysis results.

II. SPECIFICATIONS OF OBJECT

Fig. 1 shows the 3D configuration of one phase of the TFLM as a vibrator. The current direction of TFLM corresponds to the moving direction of mover, and the main flux path is in a plane perpendicular to the direction of motion. In this type of TFLM, the high power density is mainly due to high-energy PM and the saliency of mover.

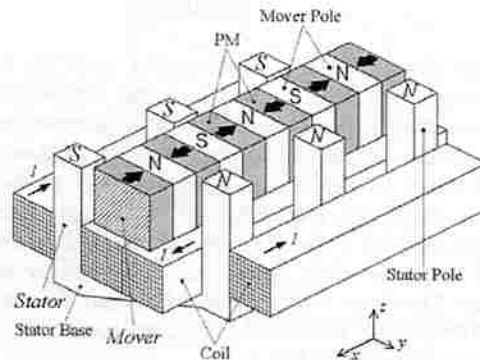


Fig. 1 The 3D Configuration

TABLE I. SPECIFICATIONS OF THE ELECTRO-DYNAMIC VIBRATOR

No. of Stator Pole	20 (pair)
No. of Mover Pole	7 (PM=8)
Stator Pole Material	50A445 (≈M27)
Mover Pole Material	50A760 (≈M45)
PM	$B_r=1.2$ (T), $\mu_r=1.05$
Rated Current	20 (A)
Rated Thrust	500 (N)
Frequency	4 (Hz)
No. of Turn	140 (turns)
Stator Length	864 (mm)
Mover Length	150 (mm)
Airgap Length	0.7 (mm)

Table 1 shows the specifications about one phase configuration and running condition. The more detailed explanation about the phase arrangement and winding magnetomotive force (*mmf*) excitation principle of this vibrator are presented in [1].

III. ANALYSIS METHODS

For using EMCN, the analysis model is divided into hexahedral shape elements according to regions. 3D EMCN is constructed by connecting the nodes of adjacent elements through permeance. The 3D analysis model is given in Fig. 2. Magnetic flux continuity has a condition that the inflow of flux is equal to the outflow of flux at node (i, j, k). From magnetic flux continuity condition as (1), system matrix (2) is constructed using equivalent *mmf* of element in magnet source region, which has linear demagnetization curve and in stator current.

$$\sum_{n=1}^6 \Phi_n = \Phi_{1,j,k} + \Phi_{2,j,k} + \Phi_{3,j,k} + \Phi_{4,j,k} + \Phi_{5,j,k} + \Phi_{6,j,k} = 0 \quad (1)$$

$$[P]\{U\} = \{F\} \quad (2)$$

where, Φ_n is the flux of nth element, $[P]$ is permeance coefficient matrix, $\{U\}$ is matrix of node magnetic scalar potential, and $\{F\}$ is forcing matrix [2][3].

To consider the end effect in mover and find the Multiple-ratio, 2D analysis model is constructed as shown in Fig. 3. Magnetic shield and imaginary magnetic flux path can substitute for stator base, which is actually 3D flux path, and these regions are analyzed by linear solution in magneto-static field while the other regions are analyzed by nonlinear solution at the same time.

IV. ANALYSIS AND MEASUREMENT RESULTS

In 2D analysis model as shown in Fig. 3, the $2\tau_p$ is the 3D analysis model length, and l_{mf} is the integral length where the thrust is not changed anymore over mover length. The Multiple-ratio is calculated by the ratio of thrust for $2\tau_p$ to thrust for l_{mf} . The equi-potential lines of the 2D analysis model are shown in Fig. 4, and the average Multiple-ratio is 3.6. The 3D analysis results are multiplied by 3.6 to get the whole thrust force for one phase of the vibrator. The thrust, which is computed from the analysis by 3D EMCN and 2D FEM, is compared with measurement results in Fig. 4.

V. CONCLUSIONS

In this paper, the effective method and the process for PM type TFLM analysis are introduced. The static thrust for mmf is computed from 3D EMCN, and then the values are multiplied by Multiple-ratio obtained by 2D FEM. The calculation results are compared with the test values, and the comparison shows the validity of the calculation method. It is expected that the computed results in this research can be used practically as reliable data to estimate the performance, and also be the reference data for design of PM type TFLM. The more detailed explanation and analysis results will be presented in the extended paper.

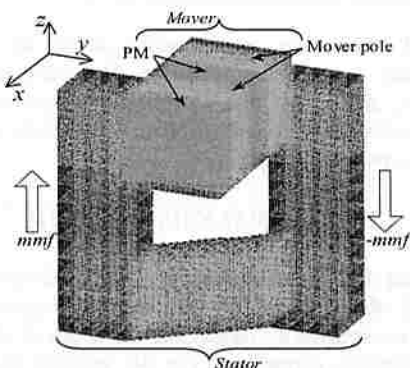


Fig. 2.5 Mesh Shape of the 3D Model

VI. REFERENCES

- [1] Tae-yun Lim, Do-Hyun Kang, Jong-Moo Kim, and Dong-Hee Kim, "A Study on control of drive for Vibrator Using PM-type Transverse Flux Linear Motor," Proceedings of the Power Conversion Conference-Osaka 2002, Vol. 1, pp43-47, 2002
- [2] Jin Hur, Dong-Seok Hyun, and Jung-Pyo Hong, "A Method for Recuotion of Cogging Torque in Brushless D.C. Motor Considering the Distribution of Magnetization by 3DEMCN," IEEE Trans., Magnetics, Vol.34, No.5, pp.3532-3535, September, 1998
- [3] Jin Hur, In-Soung Jung, and Dong-Seok Hyun, "Lateral Characteristic Analysis of PMLSM Considering Overhang Effect by 3 Dimensional Equivalent Magnetic Circuit Network Method," IEEE Trans., Magnetics, Vol. 34, No. 5, pp.3528-3531, September, 1998
- [4] Do Hyun Kang, Yeon Ho Jeong, Moon Hwan Kim, "A study on the design of transverse flux linear motor with high power density," IEEE International symposium, Industrial Electronics 2001 Proceedings, Vol. 2, No. 3, pp707-711, 2001

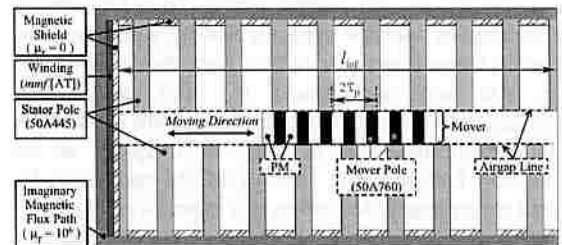


Fig. 3 2D Analysis Model with Imaginary Magnetic Flux Path

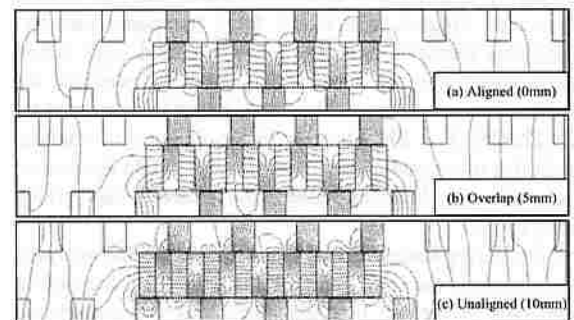


Fig. 4 Equi-potential Lines for Mover Displacement

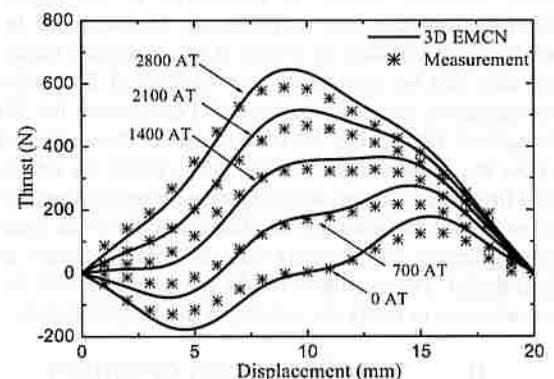


Fig. 5 Comparison of Thrusts for mmf

Thrust Calculation of Transverse Flux Linear Motor Considering End Effect of Mover

¹Ji-Young Lee, ¹Jung-Pyo Hong, Senior Member, *IEEE*, ²Do-Hyun Kang

¹Department of Electrical Engineering, Changwon National University
#9 Sarimdong, Changwon, Gyeongnam, 641-773, Korea, phone: (+8255)2625966, fax: (+8255) 2639956

²Department of Mechatronics, Korea Electrotechnology Research Institute
#28-1, Seongjudong, Changwon, Gyeongnam, 641-120, Korea, phone: (+8255)2603834
e-mail: jyecad@korea.com, jphong@changwon.ac.kr, dhkang@keri.re.kr

Abstract—This paper deals with a method for thrust calculation of a PM type transverse flux linear motor (TFLM). To perform analysis considering the 3D transverse flux path and end effect of the mover, 2D Finite Element Method (FEM) is coupled on 3D Equivalent Magnetic Circuit Network Method (EMCN). 2D analysis by FEM is used to find so-called Multiple-ratio, which is multiplied by 3D analysis results, and 3D EMCN is employed for magnetic field analysis to get the thrust of the analysis model. The calculated results are verified by comparison with measurements.

I. INTRODUCTION

Transverse Flux Linear Motor (TFLM) has so high power density per unit volume that it can reduce weight and volume of vibrator systems, and be substituted for hydraulic vibrator systems, which have disadvantages of huge size and management [1]. For design and performance assessment, however, the analysis of TFLM is more difficult than that of rotary counterparts, or the results can be inaccurate because of the end effect by limited mover length. Moreover, it is required to employ 3-dimensional (3D) analysis because of the magnetically complicated and nonsymmetrical configuration.

Therefore, this paper deals with thrust calculation of a Permanent Magnet (PM) type TFLM for a two-phase vibrator. Since this motor is used for low speed and high thrust, static thrust can also be useful data to estimate the performance of vibrator. The static thrust is calculated by 3D EMCN. For TFLM as a linear motor, the analysis method is more useful and proper than 3D FEM because of the hexahedral elementary shape and relatively fast solving time [2][3].

Considering accuracy and time required for the analysis, the vibrator is too long to model the whole construction or even only mover so that the portion of one mover-pole pair is taken as the 3D analysis model. The end effect of mover, however, cannot be considered in the model. Therefore, Multiple-ratio is required to be multiplied by the 3D analysis results as a kind of an adjustment factor. This ratio can be obtained by the analysis of 2D model with imaginary magnetic flux path [4] to consider the 3D flux path of TFLM. The 2D analysis model does not need to have the whole shape. It is enough to model the mover and a little longer stator, which is long enough to consider the mover-end leakage flux. The Multiple-ratio is not equal to either length ratio or pole ratio of analysis model to actual model. The calculated results are compared with the measurements to verify the validity of the analysis results.

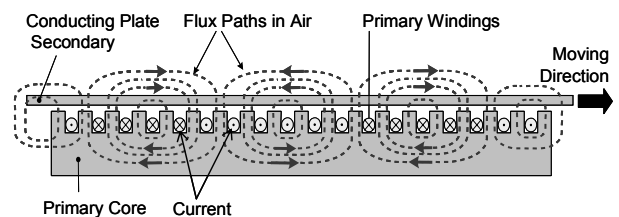
II. BASIC CONFIGURATIONS OF TFLM

Depending on the excitation, there are two distinct configurations of TFLMs as follows [5].

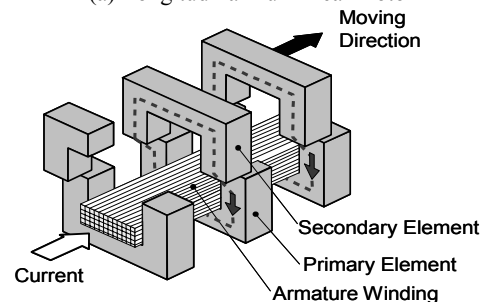
- (1) Electrically excited (TFE-LM)
- (2) Magnetically excited (TFM-LM)

The basic configuration of the TFE-LM is presented in Fig.1 in comparison with a Longitudinal Flux Linear Motor (LFLM). The primary magnetic flux of TFE-LM flows perpendicularly to the moving direction while the flux of LFLM does parallel to the moving direction. The moveable part of the TFE-LM is electrical passive and the thrust is generated based on the reluctance principle. When the primary windings are excited, the primary and secondary teeth align in opposite position.

The configuration of TFM-LM, so-called PM type TFLM in this paper and the principles of thrust force generation are shown in Fig. 2. The stator base irons are cut and developed to show the principles of force generation. The magnetic polarities between mover and stator generate the total thrust F_t in one direction. The PM type TFLM uses the PMs as excitation so that the magnetic flux density in the air gap can be amplified because the profile of the PM is bigger than the stator pole width in the air gap.



(a) Longitudinal flux linear motor



(b) Transverse flux linear motor

Figure 1. Longitudinal and transverse flux linear motors

III. ANALYSIS OBJECT

Fig. 3 shows the stator and the mover of TFLM which is fabricated for a two-phase electro-dynamic vibrator. The current direction of TFLM corresponds to the moving direction of mover, and the main flux path is in a plane perpendicular to the direction of motion.

The 3D configuration for one phase is identical to the configuration shown in Fig. 2. In this type of TFLM, the high power density is mainly due to high-energy PM and the saliency of mover. This principle is similar to spoke magnet type brushless motor [6]. In addition, it can have relatively small air gap because the attraction force can be compensated in two air gap.

Table 1 shows the specifications about one phase configuration and running conditions. The rated frequency is 4(Hz), and thrust force is 500(N). The more detail explanation about the phase arrangement and winding magnetomotive force (*mmf*) excitation principle of this vibrator are presented in [1].

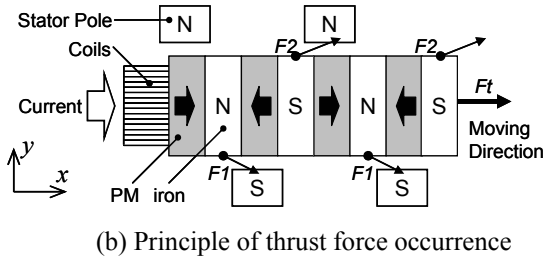
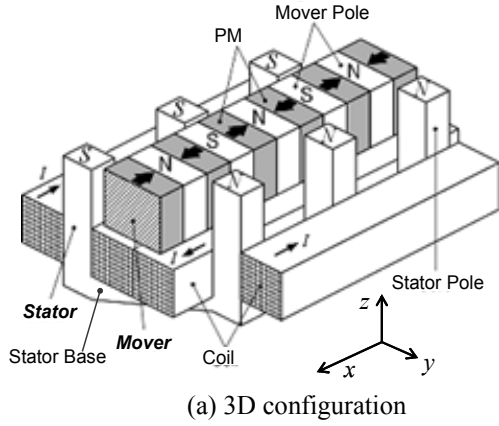


Figure 2. Configurations of PM type TFLM

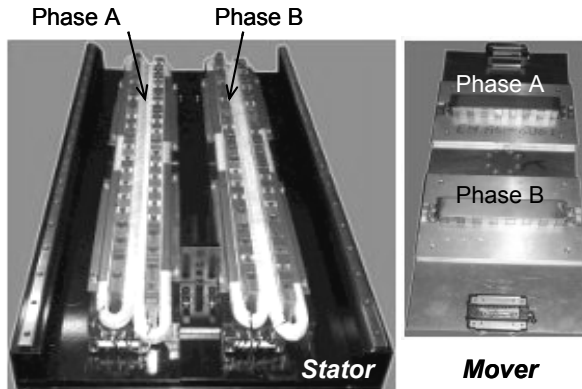


Figure 3. Fabrication of PM type TFLM

TABLE 1. SPECIFICATIONS OF THE ELECTRO-DYNAMIC VIBRATOR

No. of stator pole	20 (pair)
No. of mover pole	7 (PM=8)
Stator pole material	50A445 (\approx M27)
Mover pole material	50A760 (\approx M45)
PM	Br=1.2 (T), $\mu_r=1.05$
Rated current	20 (A)
Rated thrust	500 (N)
Frequency	4 (Hz)
No. of turn	140 (turns)
Stator length	864 (mm)
Mover length	150 (mm)
Airgap length	0.7 (mm)

IV. ANALYSIS METHODS

A. 2D Analysis by FEM

As the field variable of 2D FEM, vector potential is used in this paper, and to consider the end effect of mover and find the Multiple-ratio, 2D analysis model is constructed as shown in Fig. 4. While the 3D analysis model just reflects the original shape of the object, 2D analysis model needs more imaginary path to consider 3D magnetic flux path. For this TFLM analysis model, magnetic shield and imaginary magnetic flux path are substitutes for Stator Base actually having 3D flux path as shown in Fig. 2. Consequently the permeability of magnetic shield is about 0, and that of imaginary magnetic flux path is 10^6 as meaning of infinity. These two regions are analyzed by linear solution to keep the permeability constant in magneto-static field when the other regions are analyzed by nonlinear solution.

B. 3D Analysis by EMCN

For using EMCN, the analysis model is divided into hexahedral shape elements according to regions. 3D EMCN is constructed by connecting the nodes of adjacent elements through permeance. The 3D analysis model is given in Fig. 5. Magnetic flux continuity has a condition that the inflow of flux is equal to the outflow of flux at node (i, j, k). From magnetic flux continuity condition as (1), system matrix (2) is constructed using equivalent *mmf* of element in magnet source region, which has linear demagnetization curve and in stator current. The magnetomotive force directions of analysis model are shown in Fig. 6.

$$\sum_{n=1}^6 \Phi_n = \Phi_{1i,j,k} + \Phi_{2i,j,k} + \Phi_{3i,j,k} + \Phi_{4i,j,k} + \Phi_{5i,j,k} + \Phi_{6i,j,k} = 0 \quad (1)$$

$$[\mathbf{P}]\{\mathbf{U}\} = \{\mathbf{F}\} \quad (2)$$

where, Φ_n is the flux of nth element, $[\mathbf{P}]$ is permeance coefficient matrix, $\{\mathbf{U}\}$ is matrix of node magnetic scalar potential, and $\{\mathbf{F}\}$ is forcing matrix [2][3].

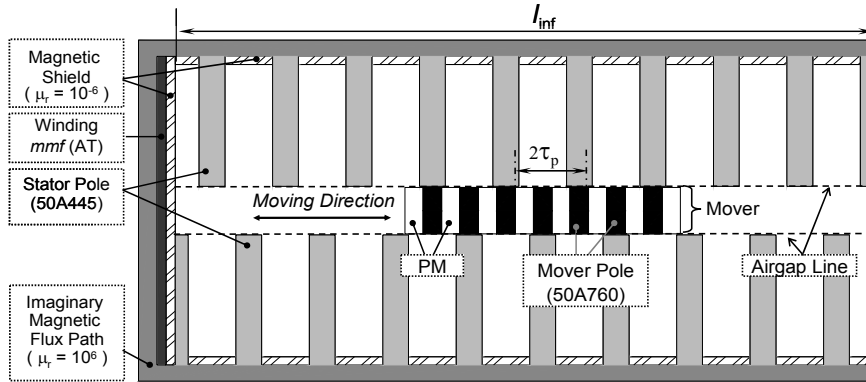


Figure 4. 2D analysis model with imaginary magnetic flux path

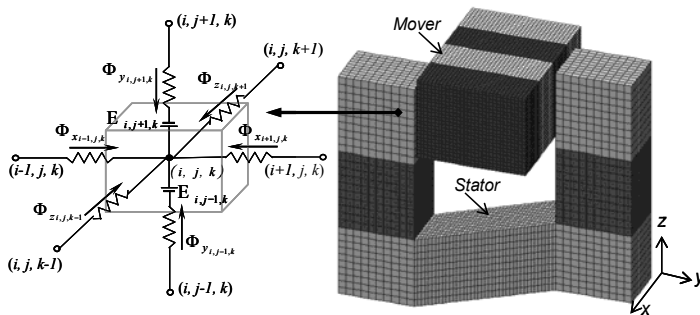


Figure 5. Conceptual model of one node in EMCN and meshed model

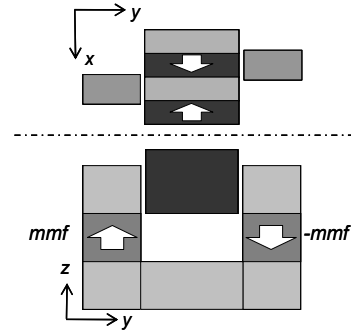


Figure 6. Magnetomotive force direction

V. Analysis and Measurement Results

A. 2D Analysis Results

Fig. 7 and Fig. 8 show the 2D analysis results by FEM. 0(mm) is the base position where mover and stator poles are aligned. Fig. 7 presents the variation of equi-potential line for mover displacement, and it shows the influence of mover-end leakage flux. Fig. 8 is thrust for mmf and integral path variation. The $2\tau_p$ is the 3D analysis model length, and l_{inf} is the integral length where the thrust does not change any more over mover length. The Multiple-ratio in Pt_M is calculated by the ratio of thrust for $2\tau_p$ to thrust for l_{inf} . The calculated results of Multiple-ratio are in Table 2.

B. 3D Analysis and Measurement Results

Thrust is calculated by 3D EMCN, and multiplied by the Multiple-ratio in Table 2.

Fig. 9 shows the thrust developed by one phase and the comparison with measurements according to current variation and mover displacement. Since the input current is considered to have ideal rectangular shape, these thrust values can be compared with static thrust measured under constant current condition. Flux linkage at all stator poles are shown in Fig. 12. With these flux data, incremental inductance can be calculated using (3).

VI. Conclusions

In this paper, the effective method and the process for PM type TFLM analysis are introduced. The static thrust for mmf is computed from 3D EMCN, and then the values are multiplied by Multiple-ratio obtained by 2D FEM. The calculation results are compared with the test values, and

the comparison shows the validity of the calculation method. It is expected that the computed results in this research can be used practically as reliable data to estimate the performance, and also be the reference data for design of PM type TFLM.

REFERENCES

- [1] Tae-yun Lim, Do-Hyun Kang, Jong-Moo Kim, and Dong-Hee Kim, "A Study on control of drive for Vibrator Using PM-type Transverse Flux Linear Motor," Proceedings of the Power Conversion Conference-Osaka 2002, Vol. 1, pp43-47, 2002
- [2] Jin Hur, Dong-Seok Hyun, and Jung-Pyo Hong, "A Method for Reduction of Cogging Torque in Brushless D.C. Motor Considering the Distribution of Magnetization by 3DEMCN," IEEE Trans., Magnetics, Vol.34, No.5, pp.3532-3535, September, 1998
- [3] Jin Hur, In-Soung Jung, and Dong-Seok Hyun, "Lateral Characteristic Analysis of PMLSM Considering Overhang Effect by 3 Dimensional Equivalent Magnetic Circuit Network Method," IEEE Trans., Magnetics, Vol. 34, No. 5, pp.3528-3531, September, 1998
- [4] Do Hyun Kang, Yeon Ho Jeong, Moon Hwan Kim, "A study on the design of transverse flux linear motor with high power density," IEEE International symposium, Industrial Electronics 2001 Proceedings, Vol. 2, No. 3, pp707-711, 2001
- [5] D. H. Kang, Y. H. Chun, and H. Weh, "Analysis and optimal design of transverse flux linear motor with PM excitation for railway traction," IEE Proc. Electr. Power Appl. Vol. 150, No. 4, pp493-499, July, 2003
- [6] J.R. Hendershot Jr, and T. J. E. Miller, Design of Brushless Permanent-Magnet Motors, Magna Physics Publishing and Clarendon Press, Oxford, 1994

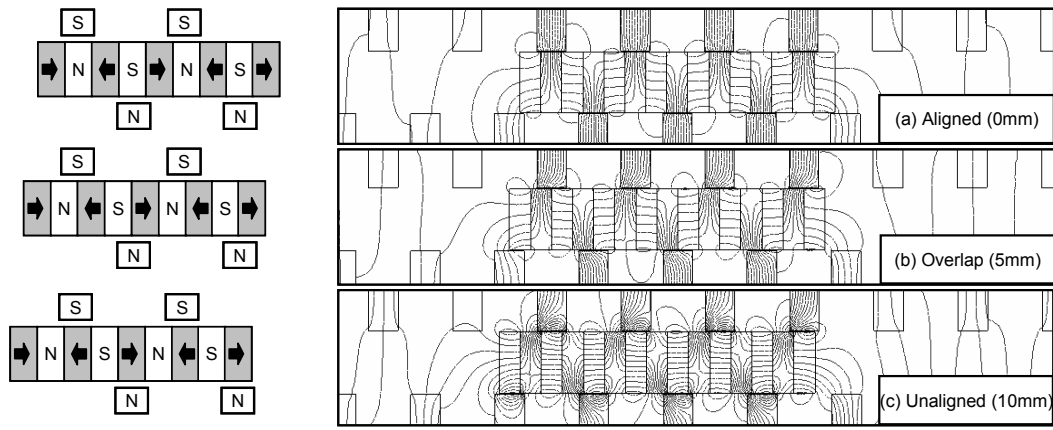


Figure 7. The top view for one phase of the TFLM

TABLE II THE MULTIPLE-RATIO OF ANALYSIS MODEL TO ACTUAL MODEL

3D EMCN Model Length	Actual Model Length	Length-ratio	Multiple-ratio
40 mm	150 mm	3.75	3.6

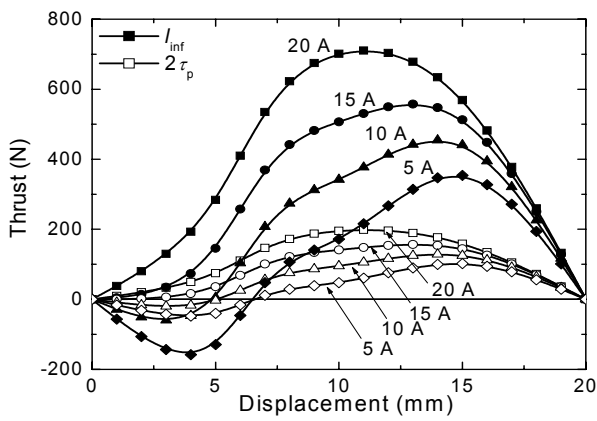


Figure 8. Thrust for input current and integral length

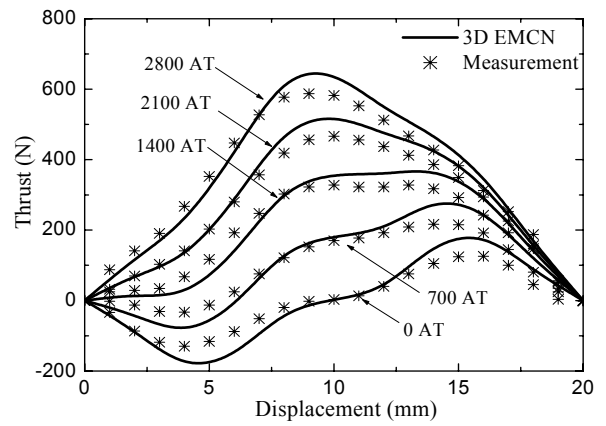
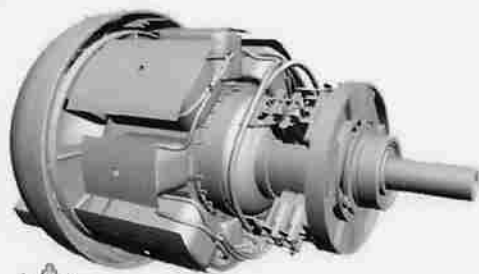


Figure 9. Comparison of thrusts for *mmf*

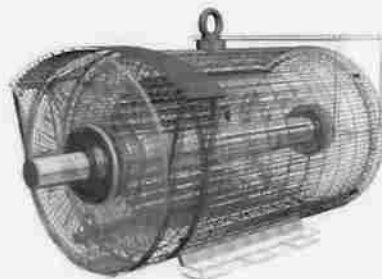
16th International Conference on Electrical Machines



ICEM 2004



5-8 SEPTEMBER 2004, CRACOW - POLAND



BOOK OF DIGESTS

vol 1

Editors: S. Wiak, M. Dems, K. Komeza

iMSI

**Institute of Mechatronics and Information Systems
Technical University of Lodz, Poland**

PS10-37	Advanced Materials for High Speed Motor Drives	935
	<i>G. Kalokiris, A. Kladas, J.A. Tegopoulos</i>	
PS10-38	Soft Magnetic Composite in Design of BLDC Motor	937
	<i>D. Miljavec, M. Zagirnyak</i>	
PS10-39	Potential of Soft Magnetic Powders for Switched Reluctance Machines in Comparison with the Laminations Solution.	939
	<i>Y. Alhassoun, C. Henaux, B. Nogaredo</i>	
PS10-40	Computer Simulation of Magnetic Field and Forces of Shell-Type Shunt Reactor 3-D Structures	941
	<i>S. Wiak, P. Drzymala, H. Welfle</i>	

Transformers, Special Machines

OS16

OS16-1	Design and Modeling of the Electric Part of an Experimental Power Plant from Sea Waves	945
	<i>N.M. Kimoulakis, S.A. Papathanassiou, A.G. Kladas</i>	
OS16-2	Improved Modeling of Three-Phase Transformer Analysis Based on Nonlinear B-H Curve and Taking into Account Zero-Sequence Flux.	947
	<i>B. Kawkabani, J.-J. Simond</i>	
OS16-3	Coupled Field, Circuit and Mechanical Model for Efficient Representation of Permanent Magnet Generator Wind Turbine.	949
	<i>A. Haniotis, A. Kladas, J.A. Tegopoulos</i>	
OS16-4	Saturation Effects in a Three-Phase Transformer Bank Composed by Single-Phase Transformers	951
	<i>C.H. Salerno, D. Bispo, J.R. Camacho</i>	
OS16-5	Analysis of a Three-Leg Core Power Transformer under Earth Fault	953
	<i>S.A. Papathanassiou</i>	
OS16-6	Avoiding the Switching-Off Failure in Capacitor Motors	955
	<i>R-N. Hasanah, M. Jufer</i>	

Use of Advanced Materials

OS17

OS17-1	Generator Behaviour of Induction Machines with Copper Die-Cast Squirrel Cage Rotor	959
	<i>N. Castéras, L. Doffe, O. Walti, J.F. Brudny</i>	
OS17-2	New Design Solution of PM Disc Motor Using SMC Material	961
	<i>G. Cvetkovski, L. Pethouska, S. Gair</i>	
OS17-3	Axial Gap Permanent Magnet DC Motor with Powder Iron Armature	963
	<i>S.M. Abu-Sharkh, M.TN. Mohammad</i>	
OS17-4	Reduction of Mass for an AC Inductor.	965
	<i>J. Saitz, A. Arkkio</i>	
OS17-5	Relationship Between Magnetization Characteristics and Torque Mechanism in High Temperature Superconducting Bulk Motor.	967
	<i>T. Nakamura, H.J. Jung, I. Muta, T. Hoshino</i>	
OS17-6	Recent Advances in Development of the Copper Motor Rotor	969
	<i>D.T. Peters, J.G. Cowie, E.F. Brush, Jr.</i>	

Linear Drives

OS18

OS18-1	Thrust Calculation of Transverse Flux Linear Motor Considering end Effect of Motor.	973
	<i>J.Y. Lee, Jung-Pyo Hong, Do-Hyun Kang</i>	
OS18-2	Analytical Procedure and Design for Transverse Flux Machines	975
	<i>Do Hyun Kang, H. Weh</i>	
OS18-3	Eddy Current Loss in Tubular Modular Permanent Magnet Machines	977
	<i>Y. Amara, J. Wang, D. Howe</i>	